FABRICATION AND STATIC TESTING OF A HIGH-SPEED MORPHING ROTOR BLADE

Zaffir Chaudhry, Andrzej Kuczek, Wenping Zhao, Sreenivasa Voleti
Raytheon Technologies Research Center, East Hartford, Connecticut, USA

Farhan Gandhi
Center for Mobility with Vertical Lift (MOVE), Rensselaer Polytechnic Institute, Troy, New York, USA

Daniel Camp
U.S. Army Combat Capabilities Development Command
Aviation & Missile Center
Fort Eustis, Virginia, USA

ABSTRACT

High-speed rotorcraft experience regions of reverse flow over the inboard sections of blades. In these regions, because of the reverse flow, the rotor blade experiences high drag, large dynamic pitching moments, and significant vibrations. If the shape of the rotor can be changed, or "morphed" in the inboard section, a number of these adverse effects can be minimized. The shape modification which provides optimum benefit between high-speed forward flight and hover was outlined in an earlier paper presented at The Vertical Flight Society's 76th Annual Forum & Technology Display [1]. This paper further builds upon the work presented at the Vertical Flight Society's 77th Annual Forum & Technology Display [2] and details the fabrication and demonstration of the full-scale rotor blade section capable of meeting the shape change requirements with adequate stiffness and stability. The fabrication of the sub-components and the final assembly of the morphing rotor blade section, which is full scale in the chordwise direction but limited in the spanwise direction, is described. The demonstrator is equipped with a rotary actuator to morph between the hover and high-speed cruise flight conditions. The morphing composite blade demonstrator meets the shape change goals while preserving stiffness and structural integrity.

1. INTRODUCTION

High speed rotorcraft experience regions of reverse flow over the inboard sections of blades. In these regions, because of the reverse flow, the rotor blade experiences high drag, large dynamic pitching moments, and significant vibrations. If the shape of the rotor can be changed, or "morphed" in the inboard section, a number of these adverse effects can be minimized. The shape modification which provides optimum benefit between high-speed forward flight and hover was outlined in an earlier paper [1]. Several geometry modifications of an 18% thick SC325218 airfoil were considered, including an ellipse, a modified ellipse, and a lower surface modified ellipse, as seen in Figure 2. The lower surface modified ellipse showed the most benefit and was also considered most practical from a structural and actuation perspective where the front spar section of the airfoil and the upper surface remains unchanged. These shapes were obtained through Reynolds Averaged Navier Stokes (RANS) simulations of flows around 2-D airfoils. While the SC325218 performed well in normal flow (from the rounded leading edge to the sharp trailing edge), large regions of separation were observed at the trailing edge on the lower surface in reverse flow conditions, seen in Figure 2. The RANS simulations in DiPalma et al [1] showed that if the lower surface shape was changed as shown in Figure 2, separation at the trailing edge was eschewed in reverse flow conditions, resulting in a significant reduction in drag. The two shapes of the selected SC325218 airfoil are more clearly shown in Figure 1.

In DiPalma et al [1] it is noted that the modified lower surface geometry results in adequate performance in normal flow conditions (on the advancing side). Thus, changes in geometry on a per/revolution basis are avoided. The proposed change in geometry also has the advantage of leaving the leading edge, as well as

Presented at the 48th European Rotorcraft Forum
Winterthur, Switzerland, 6 - 8 September 2022.

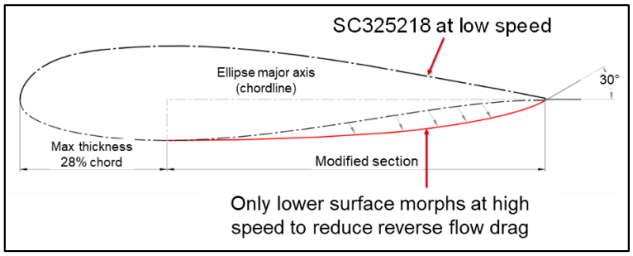

Figure 1 SC325218 airfoil section for low speed, and lower surface morphing to modified ellipse (red) for high-speed operation

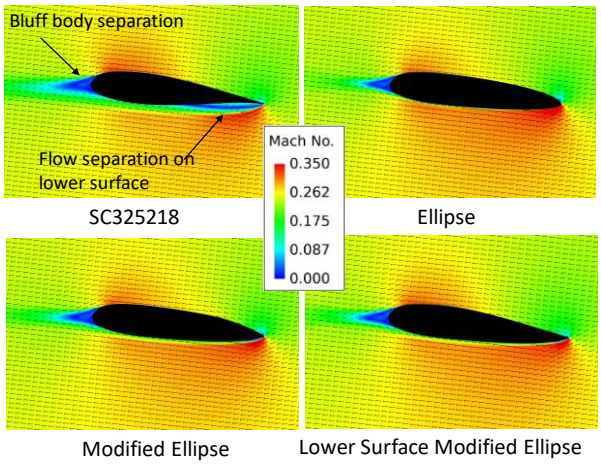

Figure 2. Flow field around various airfoils in reverse flow conditions

the upper surface of the airfoil intact. In summary, the lower surface of the baseline SC325218 is morphed as shown in Fig. 1, during high-speed cruise where large portions of the retreating side of the rotor disk experience reverse flow.

2. MORPHING ROTOR BLADE FABRICATION

Morphing (also known as adaptive) structures have been an active area of research for the last twenty years and several review papers. Barbarino et al. [3], Chillara et al. [4], Lachenal et al. [5], Qamar et al. [6] have been published summarizing the state-of-art as well as the challenges with the concepts. Some common challenges of adaptive structures, described earlier in Kuczek, et al. [2[, are recapped here for completeness. The most fundamental is the flexibility versus stiffness of the morphing structure. Stiffness requirements can be dictated by aero-elastic considerations, or simply, by the allowed deformation under aerodynamic and other maneuver loads. Flexibility, while remaining within elastic limits of the skin, is necessary to accomplish the shape change.

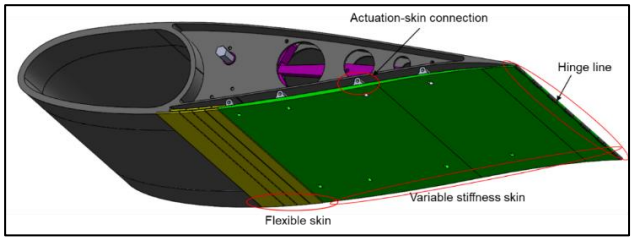

Figure 3. Concept of the 2-D morphing rotor blade. The risk areas which have been the focus of the study are highlighted with the red ring circles

Figure 4. Components fabricated for final demonstrator. Picture shows the metal ribs, morphing skin. The black plastic pieces are used only to facilitate assembly and test on a bench.

This is a delicate balance which requires the addition of some features to the typical monolithic skin. This challenge is addressed in the design described in this paper where flexibility and stiffness are simultaneously delivered to achieve the two desired shapes of the rotor blade. Another key element is the decoupling of the in-plane stiffness of the skin from the bending, i.e., allowance for the in-plane extension/contraction of the skin while undergoing bending to achieve the desired shapes. Another challenge is the efficient integration of the actuator and the kinematics within the thickness of the rotor blade. All of the above challenges are addressed by the design presented in this paper.

The fundamental morphing concept for the select rotor blade/airfoil section is shown in Fig. 3. Also highlighted in this figure are areas of fundamental research and development pertaining to morphing structures in general. A single rotary actuator is used to actuate several actuation stations, which are located within the ribs and typically spaced about 10 to 12 inches apart. It must be noted that this shape morphing takes place only in the inboard section of the blade, approximately 30% span, where the reverse flow conditions are the worst. The spar is left intact to preserve, to a large extent, the baseline bending and torsional stiffness of the blade.

Shown in Figure 4 are all the components which were fabricated. The black colored components are nonfunctional and made thru rapid prototyping process and meant only to facilitate assembly and

support. The aluminum ribs hold the kinematic linkages, hence made from metal. The flat section in the middle is the flexible skin with the co-cured stiffeners.

The flexible morphing skin, which can accommodate the bending required as well as the extension, is a very central part of the concept. It consists of a composite variable stiffness section and an in-plane flexible skin portion, located closer to the spar. These two sections serve distinct functions: the variable stiffness part of the skin allows for the requisite bending in the most deformed section closer to the training edge - this is achieved by increasing ply drop offs towards the training edge, the in-plane flexible skin, which is confined to a smaller section closer to the spar, accommodates the in-plane compression and extension required for the skin to take on the two shapes. Without incorporating this in-plane flexibility, the skin would not be able to perform the shape change function. For completeness, the skin details from Kuczek et al. [2] are shown in Figure 5. The variable stiffness skin has tailored thickness composite skin is made of carbon fiber fabric reinforced epoxy (AS4/8552). The composite thickness varies from 0.08 inches to 0.032 inches at the trailing edge. Despite the 0.032-inch thickness, this portion of the skin can withstand an order of magnitude higher pressure than expected in either of the two flow conditions. Also seen in this figure are the laser cuts that are made in the in-plane stretchable section of the skin to provide the in-plane flexibility. This happens after co-curing of all components. As a good design practice, it is best to restrict this portion of the skin to a smaller length

Shown in Figure 6 thru 8 is the skin fabrication process steps used for the final demonstrator. Prior to this, several design steps were completed, such as, anchoring the inserts to specific location on the mold, as well as, anchoring the tube to the mold. The tube forms the trailing edge hinge line. These anchors are necessary to ensure alignment between the actuation linkages and the skin D section inserts. In the current build, aluminum D-sections are also used to serve the function of skin stiffeners in between the ribs. In future designs, both the ribs and the aluminum stiffeners will be replaced with composites to reduce the weight. A key feature of this skin fabrication is the co-curing of all elements, including the variable stiffness skin. The in-plane flexible skin, the trailing tube and the spanwise stiffeners. This process provides significantly more strength and fatigue life not possible through individual adhesively bonded connections. Several strength tests have been conducted of all critical joints and found them to exceed all flight requirements.

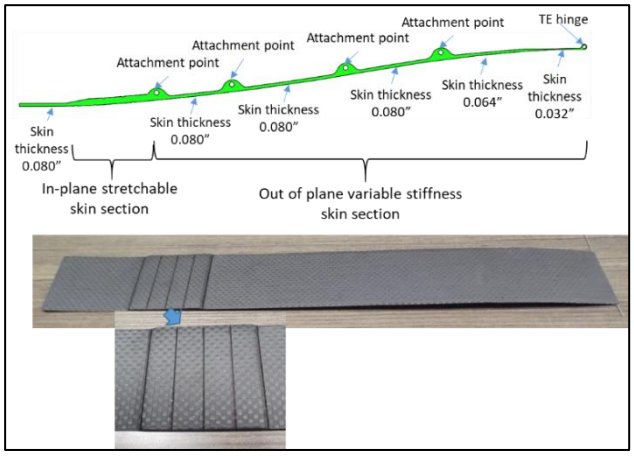

Figure 5 Cocured skin showing the variable stiffnes section as well as the in-plane streatchable section, The picture also shows the laser cuts introduced in the co-cured skin after the co-curing process

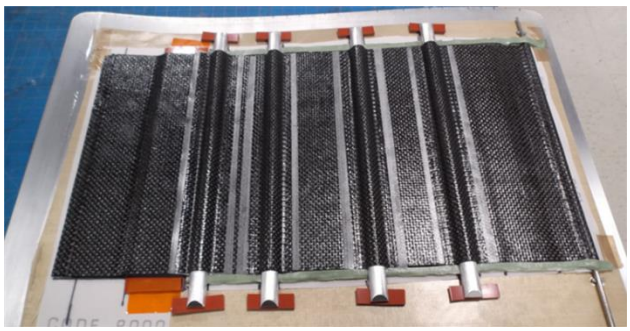

Figure 6. Composite layup of the integrated flexible skin, including stiffeners and their attachment to the mold. The ends of the low-speed shaped aluminum mold used to impart the shape to the skin, are also visible.

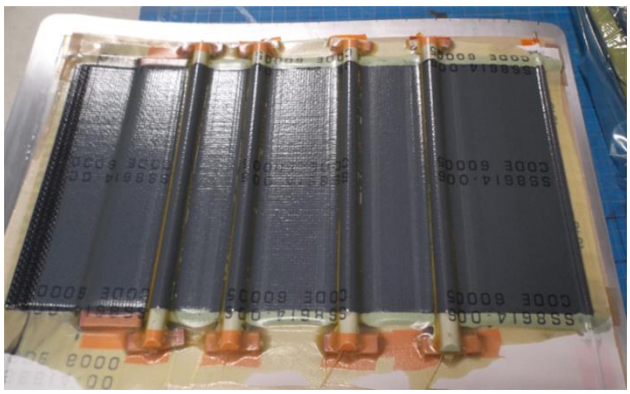

Figure 7. Cured layup, inner side of the skin is visible.

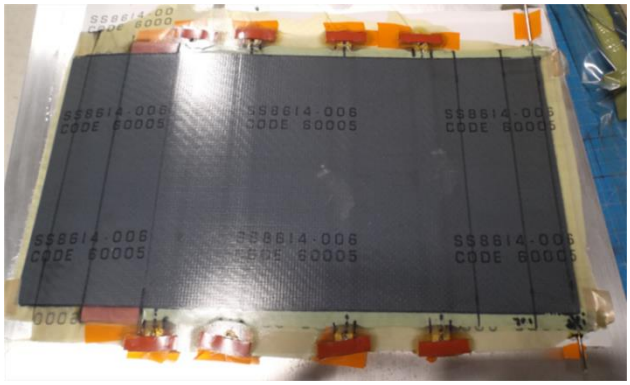

Figure 8. Cured skin – outer side, i.e., aerodyne-amically smooth side. Laser cuts have not yet been made to provide the ability to the skin to extend and contract to accommodate the change in length associated with the bending

Shown in Figure 9 is the rotary actuator and the controller which actuates both linkages through a torsion rod. This is a commercial off-the-shelf actuator used for demonstration. For flight demonstrations, light-weight flightworthy actuators, developed in earlier rotorcraft programs, capable of operation under high centrifugal load and vibration, will be used.

Shown in Figure 10 are several pictures of the demonstrator. The components used to fabricate the demonstrator have been previously shown in Figure 4 and 9. The full-scale morphing rotor, actuated by the rotary electromagnetic actuator (EMA), tracks very close to the two desired shapes (within 0.008 inches, whereas the overall out-of-plane travel of the skin in the morphing section is approximately 0.75 inches). Despite this amount of travel, the skin preserves very high bending stiffness in all regions.

Shown in Figures 11 and 12 are some close-up pictures of the trailing edge and the in-plane flexible skin section. These two technical elements are central to the concept. As can be seen clearly, the variable stiffness skin is responsible for accommodating the out-of-plane bending and the in-plane flexible skin accommodates the change in chord-wise length of the skin.

A metal tube is used to form the trailing edge hinge. This is also accommodated within the final skin co-curing process, where the composite pre-pregs are wrapped around the tube to deliver a strong connection.

Figure 9 The actuator and controller used to actuate between the two shapes

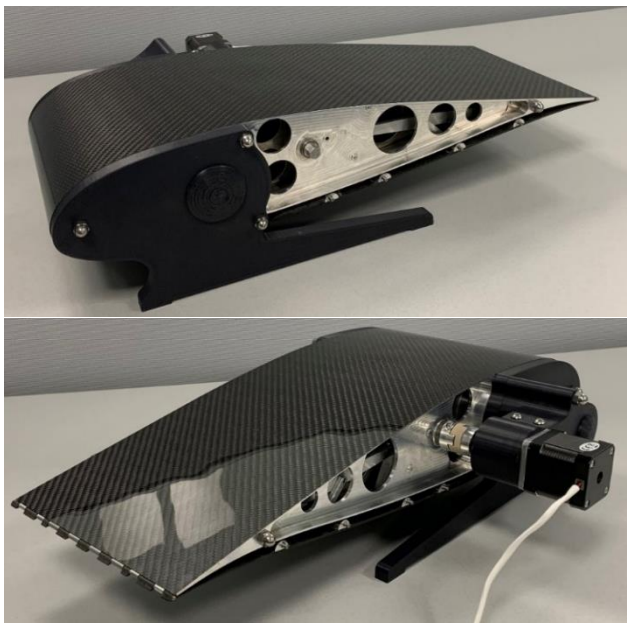

Figure 10. Pictures of the final demonstrator. The inner kinematic linkages connecting the rotary actuator's output to the aluminum stiffeners are visible through the lightening holes.

Figure 11. Showing the trailing edge of the demonstrator. The trailing edge goes through the most deformation and reversal of curvature – facilitated by the variable thickness skin in that section

Figure 12. Showing the in-plane stretchable section of the skin. The change in arc length (approx. 0.08″) is clearly visible. The laser cuts are also clearly visible in this picture.

3. TORSIONAL RIDGITY ANALAYSIS

To assess the impact of the morphing rotor geometry on the overall torsional stiffness of the rotor blade, finite element simulations were performed. These were performed for three configurations: 1) with honeycomb, i.e., baseline blade construction 2) with no honeycomb 3) no honeycomb but with ribs. The results of the analysis are summarized in Table 1.

Table 1. Rotor blade torsional stiffness derived from FE model.

	Model Parameters	Reaction Moment (in-lbs)	Torsional Stiffness (in-lb)/radian	Torsion stiffness/unit length (in-lb)/(in-radian)
1	With honeycomb	12,779.7	2,555,940	102,238
2	With no Honeycomb	11,506.8	2,301,360	92,054
3	Hollow, with 2 honeycomb ribs 1" wide	11,993.9	2,398,780	95,951
4	Hollow, with 3 honeycomb ribs 1" wide	12,071.6	2,414,320	96,573
5	Hollow, with 2 honeycomb ribs 2" wide	12,112.1	2,422,420	96,897
6	Spar only- no skin, no honeycomb or foam	10,712.6	2142520	85,701

A finite element model of a 25″ long rotor blade section was created. This uses the SC 325218 airfoil section. Material properties were assumed to be linear, elastic. The model has the graphite epoxy composite spar, glass -epoxy cover skin and Nomex honeycomb, see Figure 13. One end of the rotor section is fixed, and a rotation is applied to the other end. This constitutes the 'baseline' model. Several parametric variations were conducted on this model: i) no honeycomb, (ii) addition of 2 ribs (1″ wide), (iii) addition of 3 ribs and, (iv) two wider ribs (2″ wide).

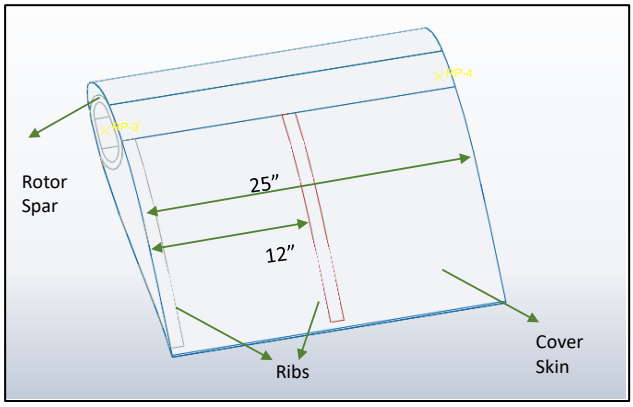

Figure 13. Geometry used for finite element analysis, shown is rotor blade structure with 2 ribs

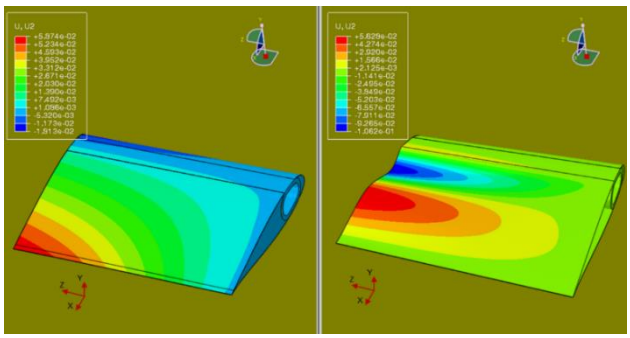

(a) with honeycomb **(b) without honeycomb**

Figure 14. Y-deflections (out-of-plane)

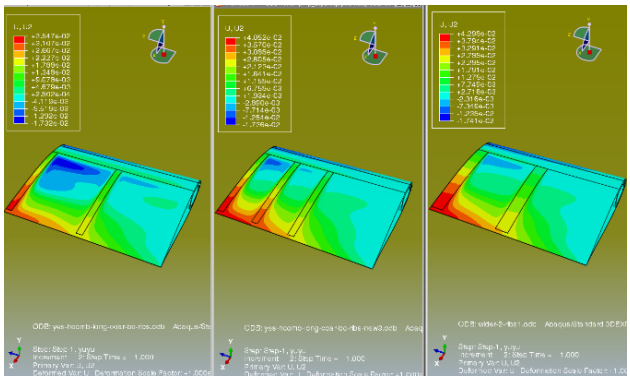

Figure 15. Y-deflections in the rotor blade model, a) with two 1" wide ribs, b) with three 1" wide ribs, c) two 2" wide ribs. (c) shows the least deflection, approximately 2 mils.

Torsional stiffness of each configuration is calculated from the results of the FE model. The torsional stiffness results (Table 1) show that most of the torsional stiffness of the rotor section comes from the spar (about 90%), which is the stiffest member in the rotor blade. Figure 14 shows the deformation of the rotor for various cases. Deflections are the highest when honeycomb is removed completely, see Figure

14b. These deflections, resulting from removal of the honeycomb, can be minimized by adding ribs, as seen in Figure 15 a, b, and c. Adding ribs reduces the skin deflection adding a third rib reduces it further. Widening the ribs has a strong influence in reducing skin deflections because it provides support where it is needed the most i.e., towards the end of the blade section where the deflections are the highest.

This analysis, confirms the fact that the debit to torsional stiffness, is minimal, however, the analysis does indicate an undue deflection, which can be minimized by the correct placement of ribs. Further, in the redesign, the space in between ribs can be filled with honeycomb, to completely alleviate all concerns. This honeycomb will reside in the upper section of the airfoil thickness where there are no kinematic linkages and motion.

4. CONCLUSIONS

A morphing rotor can reduce high speed reversed flow drag in the inboard section of the rotor. Further in the proposed concept-of-operation, the shape is only altered during the high-speed forward flight, not on a per-revolution basis. In this paper, the design and fabrication of a morphing rotor blade is presented. The static demonstrator is full scale in the chordwise direction but limited in length in the span-wise direction. The concept can be expanded to cover up to 30% of the inboard blade section where the reverse flow is most prominent. A single rotary actuator located in the inboard section can actuate a longer span of the blade. Also, in future designs, how different sections morph can be easily implemented by tailoring the section properties. Discussed in this paper are the key elements which are central to achieving a morphing structure which maintains adequate stiffness under all operational conditions. They are: 1) accommodation of in-plane strain (stretch) associated with achieving a bending profile with end constraints. The concept presented preserves bending stiffness while allowing extension compression, and further provides, several variables to achieve the right balance between extension/compression and bending stiffness 2) tailored skin stiffness (via composites) to achieve a desired shape while retaining adequate stiffness 3) co-curing of the variable stiffness skin with all embedded elements. The process of co-curing the complete skin with all components, i.e., elastomer section, embedded metal inserts and flex hinge, removes any weak joints and points of failure. 4) Kinematics which is optimized to achieve desired end shape while minimizing actuation torque requirements.

ACKNOWLEDGMENTS

This research was partially funded by the Government under Agreement No. W911W6-18-2-0005. The U.S. Government is authorized to reproduce and distribute reprints for Government purposes notwithstanding any copyright
notation thereon

REFERENCES

1. DiPalma et al. “Helicopter Rotor Morphing for Performance Improvement in Reverse Flow Conditions,” 76th Annual Forum of the Vertical Flight Society
2. Kuczek et al., “Designing a High Speed Morphing Rotor Blade”, Presented at the Vertical Flight Society’s 77th Annual Forum & Technology Display, Virtual, May10-14, 2021.
3. Silvestro Barbarino, Onur Bilgen, Rafic Ajaj, Michael Friswell and Daniel Inman, “A Review of Morphing Aircraft”, Journal of Intelligent Material Systems and Structures, Vol. 22—June 2011.
4. Chillara, V.S.C. and Dapino, M.J., 2020. “Review of morphing laminated composites”, Applied Mechanics Reviews, 72(1).
5. Lachenal, X., Daynes, S. and Weaver, P.M., 2013. “Review of morphing concepts and materials for wind turbine blade applications”, Wind energy, 16(2), pp.283-307.
6. Qamar, I.P., Groh, R., Holman, D. and Roudaut, A., 2018, April. “HCI meets material science: A literature review of morphing materials for the design of shape-changing interfaces”, In Proceedings of the 2018 CHI Conference on Human Factors in Computing Systems (pp. 1-23).
7. Fasel, U., Keidel, D., Baumann, L., Cavolina, G., Eichenhofer, M. and Ermanni, P.,” Composite additive manufacturing of morphing aerospace structures. Manufacturing Letters”, 23, pp. 85-88.